The Cryosphere Discuss., https://doi.org/10.5194/tc-2018-250
Manuscript under review for journal The Cryosphere
Discussion started: 26 November 2018

Changes in glacier facies zonation on Devon Ice Cap, Nunavut, detected from SAR imagery and field observations

Tyler de Jong[1], Luke Copland[1], David Burgess[2]
[1] Department of Geography, Environment and Geomatics, University of Ottawa, Ottawa, Ontario K1N 6N5, Canada
[2] Natural Resources Canada, 601 Booth St., Ottawa, Ontario K1A 0E8, Canada

Abstract
Envisat ASAR WS images, verified against mass balance, ice core, ground-penetrating radar and air temperature measurements, are used to map changes in the distribution of glacier facies zones across Devon Ice Cap between 2004 and 2011. Glacier ice, saturation/percolation and pseudo dry snow zones are readily distinguishable in the satellite imagery, and the superimposed ice zone can be mapped after comparison with ground measurements. Over the study period there has been a clear upglacier migration of glacier facies, resulting in regions close to the firn line switching from being part of the accumulation area with high backscatter to being part of the ablation area with relatively low backscatter. This has coincided with a rapid increase in positive degree days near the ice cap summit, and an increase in the glacier ice zone from 71% of the ice cap in 2005 to 92% of the ice cap in 2011. This has significant implications for the area of the ice cap subject to meltwater runoff.

1.0 Introduction

The Canadian Arctic Archipelago (CAA) contains the largest area of glacier ice outside of Greenland and Antarctica, representing approximately one third of global ice volume outside of the ice sheets (Dyurgerov and Meier, 2005; Radić and Hock, 2010). In recent years, glaciers and ice caps in the CAA have become a significant source of sea-level rise as anomalously high summer temperatures have caused an increase in summer melt (Gardner et al., 2011; Sharp et al., 2011; Fisher et al., 2012; Mortimer et al., 2016). For example, Jacob et al. (2012) used GRACE measurements to show that the CAA lost glacier ice at a rate of 67 +/-6 Gt a^{-1} from January 2003 to December 2010, compared to a total rate of 148 +/-30 Gt a^{-1} for all glaciers and ice caps outside of Greenland and Antarctica. Field measurements have also indicated a rapid recent acceleration in losses in the CAA, with Sharp et al. (2011) reporting mass losses at a rate of 493 kg m^{-2} a^{-1} from 2005 to 2009, five times greater than the average 1963-2004 rate. Surface mass balance (predominantly surface melt) is estimated to have accounted for 48% of total glacier mass loss from the Queen Elizabeth Islands (QEI) between 1991-2005, but 90% of total mass loss between 2005-2014 (Millan et al., 2017).

Previous studies have found a strong relationship between mass balance and glacier facies zonation (Engeset et al., 2002). Analysis of backscatter from Synthetic Aperture Radar (SAR) imagery over polar ice caps shows that relative changes in mass balance can be inferred by examining the spatial distribution of glacier facies on an annual basis (e.g., Casey and Kelly, 2010; Engeset et al., 2002; Hall et al., 2000). The large swath widths characteristic of satellite data are particularly useful for the detection and monitoring of changes in surface properties at an ice cap wide scale. For example, Casey and Kelly (2010) were able to identify the glacier ice zone, saturation/percolation zone and transient snow line on Devon Ice Cap using Radarsat-1 data. Langley et al. (2008) and Engeset et al. (2002) used Envisat ASAR and ERS 1/2 SAR imagery, respectively, to distinguish between firn and ice facies on Kongsvegen, Svalbard. The SAR-derived firn line (area where the near-surface density structure of an ice cap transitions from ice to firn) and the equilibrium line altitude (ELA) were found to have a significant relationship, suggesting that changes in the location of the SAR-derived firn line could be used as a proxy for detecting changes in relative mass balance (Engeset et al., 2002).

The aim of this study is to determine recent changes in the distribution of glacier facies across Devon Ice Cap, and use these to infer relative changes in mass balance. Facies zonation is mapped using Envisat ASAR data from 2004 to 2011, verified against results from in situ ground penetrating radar (GPR), ice core, air temperature and mass balance data. Once verified, the ASAR data provide insights into how recent changes in the spatial and temporal distribution of glacier facies across the ice cap have implications for mass balance estimates, runoff rates and densification patterns.

The Cryosphere Discuss., https://doi.org/10.5194/tc-2018-250
Manuscript under review for journal The Cryosphere
Discussion started: 26 November 2018

2.0 Study Site

Devon Ice Cap (75º10'N, 82º00'W) is one of the largest ice caps in the CAA, covering an area of ~14,400 km^2 (Fig. 1). Airborne radar measurements by Dowdeswell et al. (2004) indicated a maximum surface elevation of 1921 m a.s.l., maximum ice thickness of 880 m and an overall ice cap volume of 3980 km^3 (~10 mm sea-level rise equivalent). The main moisture source for the ice cap is provided by the North Open Water Polynya in northern Baffin Bay (Koerner, 1979; Colgan and Sharp, 2008). The geography and hypsometry of the ice cap provide an important control on the spatial distribution of accumulation and ablation rates. For example, Mair et al. (2005) found higher accumulation rates in the southeast due to the proximity of Baffin Bay, and lower rates in the northwest.

From 1959 to 2000, a comparison of aerial photography and Landsat 7 ETM+ panchromatic imagery indicated that Devon Ice Cap decreased in area by 2.4% (332 km^2), which equates to a volume loss of 67 km^3 (Burgess and Sharp 2004). Most of the decrease in areal extent occurred from the retreat of tidewater glaciers along the eastern margin and grounded portion of the stagnant southwest arm. The western basin experienced slight growth and the remaining areas showed no significant change. Abdalati et al. (2004) used airborne laser altimetry to show that between 1995 and 2000 the ice cap thickened by 0.20 m a^{-1} near the summit region, and thinned by ~0.40 m a^{-1} at lower elevations near the ice cap margins. In situ stake measurements indicate a mean annual mass balance for the NW sector of -0.341 m w.e. a^{-1} for the period 2004-2009. This rate of mass loss is almost 2 times greater than the 2000-2004 mean of -0.198 m w.e. a^{-1} and more than 4 times greater than the 1961-2003 mean of -0.082 m w.e. a^{-1} (Sharp et al., 2011; Koerner, 2005). The recent acceleration in mass losses has been attributed to anomalously warm summer temperatures and an increase in length of the melt season (Mortimer et al., 2016). Between 1963 and 2009, 58% of the total mass loss from Devon Ice Cap has occurred since 2000 (Sharp et al., 2011).

3.0 Glacier facies and SAR imagery

Snow accumulation and surface melt patterns form up to five distinct facies zones on the surface of glaciers and ice caps, determined by the density, porosity, and permeability of the surface (Benson, 1960; Muller, 1962; Koerner, 2005; Cogley et al., 2011). These typically occur from low to high elevation as follows:

The Cryosphere Discuss., https://doi.org/10.5194/tc-2018-250
Manuscript under review for journal The Cryosphere
Discussion started: 26 November 2018

The Cryosphere Discussions
Open Access

1. The *glacier ice zone* comprises the ablation area where the mass lost due to surface melting exceeds the mass gained through accumulation of snow in any particular year. In this zone solid ice is exposed at the surface each summer as the winter snowpack completely melts away.
2. The *superimposed ice zone* is located immediately above the equilibrium line altitude (ELA). Here the winter snowpack melts completely, but there is net annual accumulation due to the refreezing of meltwater at the surface.
3. The *saturation zone*, also known as the slush zone, is separated from the superimposed ice zone by a boundary termed the *firn line*. In the saturation zone the winter snowpack does not melt completely, with the snow that remains throughout the summer being transformed into firn. Here, meltwater can penetrate below the last summer surface, refreezing and resulting in internal accumulation.
4. In the *percolation zone* meltwater refreezes within the annual surface layer, but does not percolate beneath the last summer surface.
5. The *dry snow zone* is located at high elevations in the interior parts of large ice caps and ice sheets, where no melt occurs.

Winter Synthetic Aperture Radar (SAR) satellite imagery can be used to map different facies based on the intensity of backscatter (σ^0; sigma nought) of the SAR signal caused by the elementary scatterers on the glacier surface and near-surface (Fig. 2; Bardel et al., 2002; Engeset et al., 2002; Wolken et al., 2009). As discussed in more detail in the Results (Section 5.1), the glacier ice and superimposed ice zones typically have the lowest σ^0 of all facies due to the lack of reflectors at depth, the saturation and percolation zones have high σ^0 due to extensive ice layers and pipes within the firn, while the dry snow zone has low σ^0 due to the lack of internal reflectors (Partington, 1998; Langley et al., 2008). The presence of fresh dry snow above the last summer surface has a negligible impact on the reflected signal due to its low density and small crystal structure, so winter imagery is usually assumed to represent facies formed during the previous summer (Wang et al., 2007).

The Cryosphere Discuss., https://doi.org/10.5194/tc-2018-250
Manuscript under review for journal The Cryosphere
Discussion started: 26 November 2018

4.0 Data and Methods

Identification of distinct glacier facies zones on Devon Ice Cap was achieved through an integrated analysis of: 1) Envisat ASAR imagery; 2) GPR surveys; 3) shallow ice cores (<6 m); and 4) in situ measurements of surface mass balance and meteorological data. This study focuses on data collected from a transect in the northwest (Fig. 1), which was then applied to the entire ice cap and validated against independent in situ data collected in the northwest, northeast and southern sectors.

4.1 Envisat imagery

Envisat ASAR Wide Swath mode imagery (C-band, $\lambda = 5.6$ cm; pixel size 150 m, swath width 405 km) was used as it permitted complete coverage of Devon Ice Cap in a single pass. All Envisat images were acquired from descending passes with the same incidence angle, and with scene centers within 0.5° of 75.0°N, 80.4°W. This ensured that changes seen in the imagery were due to physical changes on the ice cap surface and not due to changes in satellite viewing geometry. Envisat ASAR Wide Swath Level 1b imagery was acquired for each year from 2004 to 2011 over Devon Ice Cap to observe glacier facies that developed over the previous summer (Fig. 2). All imagery was acquired from the fall and winter, when our meteorological measurements (Section 4.4) indicate that air temperatures were well below freezing, meaning that the SAR signal was unaffected by liquid water at or near the ice cap surface at the time of acquisition.

Consistent backscatter between images collected at different times during the fall and winter months was confirmed by comparing σ^0 values between scenes acquired at various time periods throughout the year after freeze-up. For example, extracted values of σ^0 from Oct. 2, 2008 and Dec. 11, 2008 images were almost indistinguishable (within 0.15 dB) from each other, providing confidence that changes in backscatter throughout the winter are due almost entirely to melt-season processes that occurred prior to freeze-up.

Envisat images were orthorectified in PCI Geomatica's OrthoEngine, where a rigorous math model and a digital elevation model (Canadian Digital Elevation Dataset; 100 m grid) were used to correct distortions due to viewing geometry and surface topography. The resulting images were radiometrically calibrated in σ^0 units (dB), output with a pixel spacing of 12.5 x 12.5 m and

The Cryosphere Discuss., https://doi.org/10.5194/tc-2018-250
Manuscript under review for journal The Cryosphere
Discussion started: 26 November 2018

projected in WGS84 UTM zone 17N. The images were imported into ESRI ArcMap 10.0, where the σ^0 values were extracted at each pixel and smoothed by applying a 50 m elevation band averaging filter across the entire ice cap.

4.2 Ground-penetrating radar

In May 2011 and 2012 a Sensors and Software™ pulseEKKO 1000 unit with 450 MHz antennae was towed behind a snowmobile across the NW transect to map the facies zones (Fig. 1). The GPR recorded for a time window of 160 ns, stack size of 16, and sample interval of 0.2 ns. Traces were recorded at 1 second interval, which equates to a distance of 1.9 m at an average travel speed of 7 km hr^{-1}. An Ashtech Z-Xtreme dual frequency GPS operating in kinematic mode was used to provide position information for each GPR trace. Post-processing of GPS data was completed through Natural Resources Canada's Precise Point Positioning service (http://webapp.geod.nrcan.gc.ca/geod/tools-outils/ppp.php?locale=en), which provides positions to ~1-2 cm horizontal and ~5 cm vertical accuracy.

The GPR data was edited and post-processed in pulseEKKO Deluxe software. A Dewow filter and Spherical and Exponential Compensation gain were applied to remove low frequency noise and amplify the signal at depth. In addition, a background subtraction (running average of 7 traces) was applied to remove repeated reflections resulting from 'ringing' of the GPR signal, and to highlight rapidly changing layers. The return from the winter snowpack was removed so that the y-axis on radargrams commenced at the last summer surface. To acquire the radar wave velocity through firn in the accumulation area, the density of an ice core collected at Dev1H (550 kg m^{-3}) was used to determine a radar wave velocity of 0.20 m ns^{-1} using the method of Kovacs et al. (1995).

4.3 Ice cores

As validation for the GPR measurements, shallow ice cores were extracted at Dev8K (1557 m a.s.l.), Dev3F (1731 m a.s.l.) and Dev1H (1781 m a.s.l.) along the northwest transect in May 2011 and 2012 (Fig. 1). Coring was conducted with a Kovacs Mark II system, which retrieved cores with a 9 cm diameter. The Dev1H and Dev3F cores ranged in length between 5.16 and 6.00 m, while the Dev8K core had a length of 3.82 m in 2011 and 4.52 m in 2012. The stratigraphy of each core was recorded first, and then the core was split into sections based on the boundaries between firn and ice layers and weighed to calculate density.

4.4 In situ surface mass balance and meteorological data

We collected measurements of in situ surface mass balance from the northwest transect and southern 'CryoSat' transect (Fig. 1). The northwest in situ mass balance network consists of 57 poles along a 60 km long transect extending from the ice cap summit region (~1800 m a.s.l.) to the terminus of the Sverdrup Glacier (~100 m a.s.l.), with a second arm extending ~15 km from 'Ice Cap Station' (ICS) at ~1300 m a.s.l. to the western margin (~1000 m a.s.l.). The CryoSat transect consists of 48 poles extending 48 km south from the summit region to the ice cap margin at ~400 m a.s.l.

The in situ mass balance was derived using the Stratigraphic System (Cogley et al., 2011), whereby mass change of the ice cap surface over the course of one year is calculated as the water equivalent (w.e.) difference between successive annual measurements of pole length above the previous end-of-summer surface. Thus, pole measurements obtained in the spring visits of year n and year n+1 provide information needed to calculate net balance for the mass balance year n-1 to year n. Height change measurements are converted to water equivalent values using the density measured at each stake, which is typically 650 – 800 kg m^{-3} in the percolation/saturation zones, 800 kg m^{-3} in the superimposed ice zone and 910 kg m^{-3} in the glacier ice zone. The location along the mass balance stake network where the annual balance transitions from positive to negative is identified as the ELA for that particular mass balance year.

On-ice air temperatures were measured throughout the period of study at four automatic weather stations at elevations of 1317 m a.s.l. (ICS), 1594 m a.s.l. (Dev7D), 1731 m a.s.l. (Dev3F), and 1781 m a.s.l. (Dev1H) (Fig. 1). Each station was equipped with a Campbell Scientific 107F thermistor with an accuracy of +/-0.4ºC, and temperatures were recorded once a minute and averaged into daily values. The thermistors were positioned ~2 m above the surface and mounted in a Gill radiation shield. The mean daily temperatures were used to calculate the annual number of positive degree days (PDD) between 2004 and 2011 at each station.

5.0 Results

5.1 Identification of glacier facies

Based on analysis of the Envisat ASAR imagery and in situ mass balance stake data, four major glacier facies zones could be delineated (Fig. 4), from high to low elevation:

(i) Dry snow zone

The dry snow zone occurs across the highest elevations of the ice cap in years when summer warmth is not sufficient to produce melt and refreezing of liquid water within or on top of the winter snowpack. This surface is a poor reflector of radar energy due to the lack of surface or internal scatterers, low snow density and small grain size (Wang et al., 2007; Partington, 1998), and is thus characterized in the Envisat ASAR imagery as areas near the ice cap summit with negative σ^0 values. Over the study period, a dry snow zone only existed on Devon Ice Cap between 2004 and 2006 (Fig. 2)

(ii) Percolation/Saturation zone

The lower elevation limit of the dry snow zone transitions into the percolation and saturation zones, which are characterized by high SAR backscatter due to vertical ice pipes and horizontal ice layers which result from meltwater that refreezes at depth within the previous winter's snowpack (Partington, 1998). Most of the scattering appears to occur at the interface between the last summer surface and base of the winter snowpack, as well as within the upper 6-11 m of firn in the form of volume scattering (Davies and Poznyak, 1993). Where volume scattering occurs, a brighter reflection is seen due to the reflection off multiple internal layers and ice features (Ulaby et al., 1986). In the Envisat ASAR imagery, these zones appear as a bright reflector and cannot be easily distinguished from each other, similar to other studies (Partington, 1998). The transitional boundary from the dry snow zone above to the percolation zone below was identified as the 0 dB level in the 2004-2006 Envisat ASAR imagery, and the percolation and saturation zones were grouped together in our analyses (Fig. 2).

We defined the lower boundary of the percolation/saturation zone as the firn line. This was readily discriminated in the ASAR imagery by a distinct contrast between the relatively bright saturation

The Cryosphere Discuss., https://doi.org/10.5194/tc-2018-250
Manuscript under review for journal The Cryosphere
Discussion started: 26 November 2018

zone at higher elevations and lower backscatter of the superimposed ice zone at lower elevations. This boundary coincided with the 0 dB Envisat σ^0 value.

(iii) Superimposed ice zone, and (iv) Glacier ice zone

The glacier ice and superimposed ice zones were identified in the SAR imagery by having the lowest backscatter of all facies, but could not be distinguished from each other using the Envisat ASAR imagery alone. σ^0 values are low in the glacier ice zone due to the lack of air and water enclosures at depth, making volume scattering negligible (Langley et al., 2007), together with large SAR signal penetration, meaning that any scattering which does occur happens at the air-surface interface (Forster et al., 1999). Backscatter is low in the superimposed ice zone because the surface there is typically smooth and contains lots of air bubbles, resulting in specular surface scattering away from the antenna.

By definition, the ELA occurs at the boundary between the superimposed ice zone above and glacier ice zone below. Due to our inability to separate these zones based solely on the Envisat ASAR σ^0 values, the transitional boundary between these zones was assigned a unique σ^0 value which corresponded to the ELA as identified from the annual in situ mass balance measurements collected from the NW transect. We then classified all regions below the prescribed ELA σ^0 value as glacier ice, and regions between the ELA σ^0 value and 0 dB firn line as superimposed ice. Although the glacier ice zone was predominately characterized as having low σ^0 values, note that some specular returns below the ELA caused higher σ^0 values particularly over rough surfaces (e.g., crevasses) and variable geometry.

5.2 Validation of glacier facies delineations

Validation of the glacier facies boundaries for each year of this study was based on comparisons with complementary in situ data collected from three main regions of the ice cap (Fig. 1): 1) surface air temperature, GPR, ice core and meteorological data collected from the northwest basin; 2) GPR transects surveyed by Sylvestre et al. (2013) across the northeast sector; 3) in situ surface mass balance stake data, and GPR data, collected along the Cryosat transect in southerly parts of the ice cap by Gascon et al. (2013).

5.2.1 Northwest validation (GPR, ice cores and meteorological data)

GPR profiles collected along the northwest transect in 2011 and 2012 show clear changes in near-surface returns at the boundary between regions dominated by low backscatter and high ice content at low elevations (i.e., glacier ice/superimposed ice zones) vs. regions dominated by high backscatter and high firn content at higher elevations (i.e., saturation/percolation zones; see Fig. 3). The dominant ice composition of the core retrieved from Dev8K (1557 m a.s.l.) in May 2011 supports this interpretation (Fig. 3a). Comparing the May 2011 GPR profile with the Envisat imagery acquired in the same winter (Oct. 7, 2010) provides clear discrimination between the glacier ice/superimposed ice and saturation/percolation zones (Fig. 3b). In this image, the location of the firn line on the GPR radargram occurs at the location of the 0 dB σ^0 value, which directly corresponds to the abrupt down-glacier transition from high to low backscatter in the Envisat image (Fig. 3c). This pattern was also true for the May 2012 GPR radargram and associated ice cores when compared with the Nov. 17, 2011 Envisat image.

Air temperature data collected from the northwest transect provides evidence supporting the presence of an occasional pseudo dry snow zone in the vicinity of the ice cap summit. As shown in Fig. 2, a region of low backscatter was present in this region between 2004 and 2006 at a time when air temperature records indicate limited melt. In 2004 annual PDDs were zero at Dev1H (1781 m a.s.l.) and Dev3F (1731 m a.s.l.), and only 4ºC at ICS (1317 m a.s.l.). At Dev1H, annual PDD values were 1ºC in 2005 and 7ºC in 2006, respectively. The melting intensity for these years was likely insufficient to produce ice pipes and lenses within the snowpack that would enhance backscatter, thus resulting in low backscatter values and a clear contrast with the percolation zone below. However, the presence of some melt eliminates this region from the true definition of a dry snow zone by Benson (1960), making use of the term ‘pseudo dry snow zone’ more appropriate.

5.2.2 Northeast validation (GPR data)

Three 500 MHz GPR profiles undertaken in the northeast sector of the Devon Ice Cap in May 2008 by Sylvestre et al. (2013; their Fig. 5) were used to map the glacier facies, with verification provided by density and surface composition recorded in five boreholes and a range of snow density pits and snow depth measurement points. Their GPR profiles showed the firn line to be located at 1264, 1271, and 1275 m a.s.l., which compares well with the Envisat firn line of 1250-

1300 m a.s.l. determined from the location of the 0 dB σ^0 value in the winter 2007/8 (Nov. 22, 2007) Envisat imagery.

5.2.3 CryoSat transect validation (GPR and in situ mass balance data)

500 MHz GPR profiles collected along the CryoSat transect from 2007 to 2012 by Gascon et al. (2013), hereafter referred to as G2013, provide validation of the glacier facies derived in this study, but also highlight issues with their published results. The G2013 profiles were collected during the spring (i.e., April/May), before the onset of summer melt, and therefore correspond to the near surface density of the ice cap that developed during the previous summer melt season. For comparisons with the glacier facies derived from Envisat in this study, the GPR profiles collected by G2013 will therefore be referred to as the year in which the glacier facies developed, which is the year prior to that stated in their paper.

For the entire period of overlap between the two studies (i.e., 2006-2011), the firn line, or upper limit of the superimposed ice zone, as reported by G2013 was on average 90 m lower in elevation (~3 km horizontal separation) than the Envisat-derived firn line identified by the 0 dB σ0 value (Fig. 5). The largest difference occurred in 2006 when the G2013 firn line was 140 m lower in elevation than the Envisat firn line (~5 km horizontal separation), while the best agreement occurred in 2011 when the firn lines were virtually co-located with only a 15 m difference in elevation. The largest discrepancy in 2006 coincided with the lowest in situ ELA recorded throughout the 6-year period of study, while the smallest difference in 2011 coincided with the highest in situ ELA. This relationship suggests an increased reliability in detecting the firn line in ASAR imagery under high melt conditions, which is likely due to stronger contrast in backscatter between the percolation/saturation zone and superimposed ice/glacier ice zone.

Further comparisons reveal large discrepancies between the Envisat ELA for the CryoSat transect (derived by applying the unique σ^0 value at the superimposed/glacier ice zone boundary from in situ mass balance measurements in the northwest transect), and that derived in G2013 (Fig. 5). For all five years of measurement from 2006 to 2011 (excluding 2007), the G2013 ELA was interpreted to be a constant value of ~1120 m a.s.l., which was on average ~260 m lower than the Envisat ELA values. The maximum difference was in 2011, when the G2013 ELA was 460 m lower than

The Cryosphere Discuss., https://doi.org/10.5194/tc-2018-250
Manuscript under review for journal The Cryosphere
Discussion started: 26 November 2018

the one derived in this study (Fig. 5). A similar discrepancy occurred between the G2013 ELA and the in situ ELA derived from mass balance stake measurements along the Cryosat transect, with the G2013 ELA being on average 360 m lower for the 2006-2011 period, with a maximum difference (G2013 ELA lower) of 511 m in 2011. Close agreement (77 m average) between the in situ ELA derived along the CryoSat transect and the corresponding Envisat ELA suggests that the assumption of a constant ELA by G2013 is unrealistic.

5.3 Changes of glacier facies, 2005-2011

Using the definitions described above, the location of the firn line and ice-cap wide extent of each facies was calculated for the 2005 to 2011 Envisat scenes (Fig. 4). This could not be done for the 2004 scene due to the lack of clear boundaries between facies (Fig. 2); this year was unusually cold, with an ELA of 1090 m a.s.l., positive summer mass balance at elevations down to 1317 m a.s.l., and observations in snow pits near the ice cap summit indicating that the last summer surface was poorly developed. The pseudo dry snow zone was therefore extensive in 2004, meaning that it could not be easily distinguished from the glacier ice and superimposed ice zones in the Envisat imagery. In this case, the summer surface from the year before is likely depicted in the Sept. 23, 2004, Envisat image due to the lack of surface scatterers in the last summer surface, meaning that the firn line in that image likely indicates the 2003 firn line.

On the northwest transect the Envisat firn line increased in elevation from 1555 to 1685 m a.s.l. between 2005 and 2011 (Fig. 6). This equates to a rate of 27 m a^{-1}, compared to a rise in the in situ derived ELA of 44 m a^{-1} on the northwest transect over the same period, resulting in a reduction in area of the superimposed ice zone (Fig. 4b).

From 2004 to 2006 at elevations of 1300-1350 m a.s.l. (near the ELA) along the northwest transect, σ^0 increased from -2.2 to -1.4 dB (Fig. 7a). This is seen alongside an increase in annual PDDs recorded at ICS (1317 m a.s.l.) from 4ºC to 44ºC (Fig. 7a), and a decrease in the net mass balance at this station from +0.20 m w.e. a^{-1} to -0.06 m w.e. a^{-1} (Fig. 7b). A subsequent decrease in σ^0 from -1.4 to -2.1 dB between 2006 and 2011 occurred in conjunction with a period of higher PDDs than were observed between 2004 and 2006, and an increasingly negative surface mass balance (Fig. 7b). The backscatter pattern is indicative of an increase in near-surface scatterers (e.g., ice lenses, pipes) from 2004 to 2006, followed by a decrease in surface scatterers as this region became part of the glacier ice/superimposed ice zone after 2006.

The glacier ice zone generally increased in both area and maximum elevation from 2005 to 2011, with large up-glacier migrations between 2007-2008 and 2010-2011 (Fig. 4a). In 2005 the glacier ice zone occupied 71% (10,282 km^2) of Devon Ice Cap. This zone increased to 85% (12,189 km^2) of the ice cap in 2008 and 90% (12,971 km^2) in 2011 (Fig. 4b). The superimposed ice zone decreased in extent as air temperatures (PDDs) were sufficient to cause surface melt at elevations between the ELA and firn line from 2005 to 2011, with particularly warm summers in 2008 and 2009 (Fig. 7a). This is indicative of the ELA 'catching-up' to the firn line as increased melt rates acted to infill pore space in the lower firn facies zones. This is seen as a consequence of the differing migration rates to higher elevation between the ELA and firn line (Fig. 6).

For the years 2005, 2006 and 2007, the percolation/saturation zone grew to cover 8%, 16%, and 18% of the ice cap, respectively, as a result of the decline of the pseudo dry snow zone. The pseudo dry snow zone, defined as the total ice cap area above the saturation/percolation zone with σ^0 values <0 dB, had a spatial extent of 723 km^2 in 2005 and 323 km^2 in 2006, but became nonexistent from 2007 onwards (Fig. 4). The percolation/saturation zone subsequently decreased in area from 2008 to 2011 (13%, 13%, 9% and 8% of total ice cap area) due to the progression of the glacier ice zone to higher elevations (Fig. 4b). The zone of peak backscatter has been increasing in elevation since 2004, indicating that higher elevation areas are experiencing more melt.

The σ^0 value from 1750-1800 m a.s.l. along the northwest transect changed from <0 dB in 2004 and 2005 (-0.5 and -0.4 dB) to >0 dB (0.4 to 1.2 dB) from 2006 to 2011. To assess controls on the σ^0 values, they were correlated with PDDs, previous winter accumulation, and surface mass balance recorded from the mass balance stake and weather station at 1781 m a.s.l. (Fig. 8). The change in σ^0 values appear to be related to all of these factors, although only the relationship between σ^0 and PDDs is statistically significant at the 95% level.

Changes in spatial extent of the glacier facies zones are also closely linked to the ice cap topography. For example, the southern portion of Devon Ice Cap, which is characterized by

The Cryosphere Discuss., https://doi.org/10.5194/tc-2018-250
Manuscript under review for journal The Cryosphere
Discussion started: 26 November 2018

relatively low surface slopes (average 1.4º over a 23 km transect south of the summit), has seen the largest areal expansion of the glacier ice zone (Fig. 4). By contrast, the steeper northeast portion (average surface slope 2.3º over a 23 km transect NE of the summit) has experienced smaller glacier facies zone migration.

6.0 Discussion

This study has demonstrated that Envisat ASAR imagery can be used to distinguish three distinctive glacier facies zones on Devon Ice Cap: (1) a glacier/superimposed ice zone, (2) a saturation/percolation zone, and in cold years, (3) a pseudo dry snow zone. These were identifiable in the SAR imagery using spatial variations in backscatter values, similar to several previous studies (Engeset et al., 2002; Langley et al., 2008; Casey and Kelly, 2010). It was not possible to distinguish the superimposed ice zone from the glacier ice zone in the SAR imagery alone, similar to the finding of Casey and Kelly (2010), although the extraction of the σ^o value at the in situ ELA still allowed for mapping of its annual distribution between there and the Envisat-derived firn line. GPR transects from the northern half of Devon Ice Cap provided information on the near-surface stratigraphy of the ice cap (i.e., ice vs. firn), which was confirmed by shallow ice cores. This information provided useful validation of the backscatter signal in Envisat imagery, with the position of the firn line identifiable in both the ground and satellite measurements.

Comparison of facies zone boundaries derived from other studies provides insight into the accuracy of the glacier zones derived in this work. Comparisons with glacier facies mapped by Gascon et al. (2013) solely from 500 MHz GPR surveys along the Cryosat line were limited to the upper and lower limits of the superimposed ice zones due to differences in the classification schemes used between the studies. There was relatively good agreement between the firn line (i.e., saturation/percolation vs. superimposed ice zone boundary) for the years 2006, 2008, 2009 and 2010 (average difference = 91 m, st. dev. = 58 m), but there was significant discrepancy in locating the superimposed / glacier ice zone boundary, or ELA (average difference = 260 m, st. dev. = 141 m) between studies. Data from the in situ mass balance surveys conducted along the CryoSat line showed close agreement between the ELA and the lower superimposed ice zone derived in this study, but relatively poor agreement with Gascon et al. (2013) (average difference = 360 m, st.

dev. = 230 m), indicating that the lower superimposed ice zone was mapped with greater accuracy in this study.

Comparisons between the 2005 facies boundaries derived over Devon Ice Cap by Wolken et al. (2009), who used post-melt season QuikSCAT scatterometer data from 1999-2005, indicated that their boundaries are an average ~850 m lower compared to the same facies boundaries derived in this study. Similarly, the Wolken et al. (2009) ELAs were placed ~600 m lower than the in situ derived ELAs, which suggests a significant misinterpretation of the dominant facies boundaries from their QuikSCAT data.

During the period of this study, changing patterns of backscatter in the Envisat imagery over the surface of Devon Ice Cap clearly highlight the migration of the dominant glacier facies. Mass balance and temperature data between 1300 and 1600 m a.s.l. indicate that melt rates increased from 2004 to 2006 (Fig. 6a), which likely resulted in the presence of more ice lenses and associated increases in backscatter. After a peak backscatter value in 2006, a gradual decrease in σ^0 was seen alongside an increase in PDDs and a physical transformation of this region of the ice cap from an accumulation area with high backscatter (firn facies), to an ablation area with low backscatter (glacier/superimposed ice facies). This observation is consistent with Engeset et al. (2002), who found that in negative mass balance years on Kongsvegen Glacier, Svalbard, firn facies areas near the ELA can transform into superimposed or glacier ice zones.

Our results indicate that Envisat ASAR imagery is sensitive to annual fluctuations in surface mass balance, with significant inter-annual variability that is reflective of annual changes in surface conditions. The effect of penetration of the Envisat SAR signal by up to several meters into the surface layers of firn and ice therefore appears to be of less importance than annual changes in near-surface conditions. The one exception is for years with strongly positive mass balance conditions, such as 2004, when little surface melt is present and facies become indistinguishable and/or dominated by conditions from previous year(s).

7.0 Conclusions

Upglacier migration of the firn line has significant implications concerning firn densification and mass loss due to summer runoff from Arctic ice caps. The location of the runoff limit is a function of the firn line (Braithwaite et al., 1994), meaning that as the firn line increases in elevation, a greater area of the ice cap loses mass due to runoff that would otherwise percolate vertically downwards and refreeze in the near-surface firn. Sufficient melt and refreezing within the firn pack will result in an increase in densification as melt refreezes within the porous firn facies (Braithwaite et al., 1994), creating impermeable surface layers that act to enhance runoff from the ice cap (Pfeffer et al., 1991). If the firn line is assumed to be the runoff limit, which Braithwaite et al. (1994) say lie fairly close together, then in summer 2012 it is likely that ~92% of the total area of Devon Ice Cap (i.e., extent of the glacier ice zone in Nov. 2011; Fig. 4) lost its winter accumulation to run-off.

Changing conditions of near-surface firn detected from the Envisat imagery also provide valuable insight into the impacts of recent warming on the highest elevation regions of Devon Ice Cap. The lack of summer melt at high elevations (>1700 m a.s.l.) from 2004 to 2006 was the likely cause of low backscatter values near the ice cap summit, enabling this region to be classified as part of the pseudo dry snow zone (since the 1960s this zone has only been an intermittent phenomenon at the summit; Koerner, 2005). From 2006 to 2011, Envisat ASAR σ^0 results show a transition from a pseudo dry snow zone to a saturation/percolation zone across the summit region. The elimination of the pseudo dry snow zone was followed by a decrease in the saturation/percolation zone as the firn line continued to migrate to higher elevations. While these changes do not have an immediate impact on the mass balance of the ice cap, they do improve our understanding of the extent of enhanced firn densification (Gascon et al., 2014), and aid in interpreting elevation changes across these regions from airborne and satellite altimetry.

Results from our analysis of inter-annual variability in glacier facies reveal an increase in elevation of the firn line, associated with the elimination of a pseudo dry snow zone and an upslope migration of the glacier and superimposed ice zones over Devon Ice Cap from 2004 to 2011. From 2006 to 2011, for example, up-slope migration of the firn line progressed ~6 km in the northwest sector. This has expanded the surface area vulnerable to mass loss due to meltwater runoff. This is reflected in the fact that ice core records from Devon Ice Cap show an increase in melt features and consequent densification at high elevations since the mid-1990s (Fisher et al., 2012; Colgan and Sharp, 2008). For example, Bezeau et al. (2013) used a total of 54 shallow cores from the Cryosat line on Devon Ice Cap to identify the upward migration of the upper limit of >1 m thick ice layers from ~1300 to ~1550 m a.s.l. over the period 2004 to 2012, with the density of the top 2.5 m of the firn increasing by 36% over this period. If the 2004 to 2011 trend in glacier facies zonation continues, Devon Ice Cap will become similar in form to more southerly ice caps such as Barnes, where summer melt is so intense that there is no annual firn accumulation, and accumulation only occurs through superimposed ice (Dupont et al., 2012). In effect, these mid-arctic ice caps may be a precursor to changes that will eventually occur on Devon Ice Cap.

Acknowledgements

We thank the Natural Sciences and Engineering Research Council of Canada, Northern Scientific Training Program, University of Ottawa, Ontario Graduate Scholarship, Canada Foundation for Innovation and Ontario Research Fund for assistance with funding to complete this project. We also thank the Polar Continental Shelf Program (Natural Resources Canada) for logistic support and the Nunavut Research Institute and the communities of Grise Fiord and Resolute Bay for permission to conduct research on Devon Ice Cap. Support for D.O. Burgess was provided through the Climate Change Geoscience Program, Earth Sciences Sector (contribution number 20140321), Natural Resources Canada.

References

Abdalati, W., Krabill, W., Frederick, E., Manizade, S., Martin, C., Sonntag, J., Swift, R., Thomas, R., Yungel, J., and Koerner, R. (2004). Elevation changes of ice caps in the Canadian Artic Archipelago. *Journal of Geophysical Research*, **109**(F04007).

Bardel, P., Fountain, A., Hall, D. and Kwok, R. (2002). Synthetic aperture radar detection of the snowline on Commonwealth and Howard Glaciers, Taylor Valley, Antarctica. *Annals of Glaciology*, **34**, 177-183.

Benson, C. (1960). Stratigraphic studies in the snow and firn of the Greenland ice sheet. *Dissertation (Ph.D.)* California Institute of Technology

Bezeau, P., Sharp, M., Burgess, D. and Gascon, G. (2013). Firn profile changes in response to extreme 21st-century melting at Devon Ice Cap, Nunavut, Canada. *Journal of Glaciology*, **59**(217), 981-991.

Braithwaite, R., Laternser, M., and Pfeffer, T. (1994). Variations of near-surface firn density in the lower accumulation area of the Greenland ice sheet, Pikitsoq, West Greenland. *Journal of Glaciology*, **40** (136), 477-485.

Brown, I. (2012). Synthetic Aperture Radar Measurements of a retreating Firn Line on a Temperate Icecap. *IEEE Journal of selected Topics in Applied Earth Observations and Remote Sensing*, **5**(1), 153-160.

Burgess, D. and Sharp, M. (2004). Recent Changes in Areal Extent of the Devon Ice Cap, Nunavut, Canada. *Arctic, Antarctic, and Alpine Research*, **36(**2), 261-271.

Casey, JA. and Kelly, R. (2010). Estimating the equilibrium line of Devon Ice Cap, Nunavut, from RADARSAT-1 ScanSAR wide imagery. *Canadian Journal of Remote Sensing*, **36**(1), S41-S55.

Cogley, J.G., Hock, R., Rasmussen, L.A., Arendt, A.A., Bauder, A., Braithwaite, R.J., Jansson, P., Kaser, G., Möller, M., Nicholson, L. and Zemp, M. (2011). Glossary of Glacier Mass Balance and Related Terms, IHP-VII Technical Documents in Hydrology No. 86, IACS Contribution No. 2, UNESCO-IHP, Paris.

Colgan, W. and Sharp, M. (2008). Combined oceanic and atmospheric influences on net accumulation on Devon Ice Cap, Nunavut, Canada. *Journal of Glaciology*, **54**(184), 28-40.

Davies, C. and Poznyak V. (1993). The depth of penetration in Antarctic firn at 10 GHz. *IEEE Transactions in Geoscience Remote Sensing*, **31**(5), 1107-1111.

Dowdeswell, J.A., T.J. Benham, M.R. Gorman, D. Burgess and M. Sharp. (2004). Form and flow of the Devon Island ice cap, Canadian Arctic. *Journal of Geophysical Research*, **109**, 1-14.

Dupont, F., Royer, A., Langlois, A., Gressent, A., Picard, G., Fily, M., Cliche, P. and Chum, M. (2012). Monitoring the melt season length of the Barnes Ice Cap over the 1979-2010 period using active and passive microwave remote sensing data. *Hydrological Processes*, **26**, 2643-2652.

Dyurgerov, M. and Meier, M. (2005). Glaciers and the changing earth system: A 2004 snapshot. *Institute of Arctic and Alpine Research: University of Colorado Boulder*. Occasional Paper 58.

Engeset, R., Kohler, J., Melvold, K., and Lunden, B. (2002). Change detection and monitoring of glacier mass balance and facies using ERS SAR winter images over Svalbard. *International Journal of Remote Sensing*, **23**(10), 2023-2050.

Fisher, D., Zheng, J., Burgess, D., Zdanowicz, C., Kinnard, C., Sharp, M. and Bourgeois, J. (2012). Recent melt rates of Canadian arctic ice caps are the highest in four millennia. *Global and Planetary Change*, 84-85, 3-7.

Forster, R., Jezek, K., Bolzan, J., Baumgartner, F. and Gogineni, S. (1999). Relationships between radar backscatter and accumulation on the Greenland ice sheet. *International Journal of Remote Sensing*, **20**(15-16), 3131-3147.

Gardner, A., Moholdt, G., Wouters, B., Wolken, G., Burgess, D., Sharp, M., Cogley, G., Braun, C. and Labine, C. (2011). Sharply increased mass loss from glaciers and ice caps in the Canadian Arctic Archipelago. *Nature*, **473**(7347), 357-360.

Gascon, G., Sharp, M., Burgess, D., Bezeau, P. and Bush, A.B.G. (2013). Changes in accumulation-area firn stratigraphy and meltwater flow during a period of climate warming: Devon Ice Cap, Nunavut, Canada. Journal of Geophysical Research Earth Surface, 118(4), 2380-2391.

Gascon, G., Sharp, M., Burgess, D., Bezeau, P., Bush, A.B.G., Morin, S., and Lafaysse, M. (2014). How well is firn densification represented by a physically-based multi-layer model? Model evaluation for the Devon Ice Cap, Nunavut, Canada. *Journal of Glaciology*, **60**, 694-704.

Hall, D., Williams Jr., S., Barton, J., Sigurdsson, O., Smith, L. and Garvin, J. (2000). Evaluation of remote-sensing techniques to measure decadal-scale changes of Hofsjokull ice cap, Iceland. *Journal of Glaciology*. **46**(154), 375-388.

Jacob, T., Wahr, J., Pfeffer, T. and Swenson, S. (2012). Recent contributions of glaciers and ice caps to sea level rise. *Nature*, **482**, 514-518.

Koerner, R. (1979). Accumulation, ablation and oxygen isotope variations on the Queen Elizabeth Islands ice caps, Canada. *Journal of Glaciology*, 22(86), 25-41.

Koerner, R. (2005). Mass balance of glaciers in the Queen Elizabeth Islands, Nunavut, Canada. *Annals of Glaciology*, **42,** 417-423.

Kovacs, A., Gow, A.J. and Morey, R.M., 1995. The in-situ dielectric constant of polar firn revisited. *Cold Regions Science and Technology*, **23**(3), 245-256.

Langley, K., Hamran, S.-E., Hogda, K.A., Storvold, R., Brandt, O., Hagen, J.O. and Kohler, J. (2007). Use of C-band ground penetrating radar to determine backscatter sources within glaciers. *IEEE Transactions on Geoscience and Remote Sensing*, **45**(5), 1236-1246.

Langley, K., Hamran, S.-E., Hogda, K.A., Storvold, R., Brandt, O., Kohler, J. and Hagen, J.O. (2008). From Glacier Facies to SAR Backscatter Zones via GPR. *IEEE Transactions on Geoscience and Remote Sensing*, **46**(9), 2506-2515.

Mair, D., Burgess, D. and Sharp M. (2005). Thirty-seven year mass balance of Devon Ice Cap, Nunavut, Canada determined by shallow ice coring and melt modeling. *Journal of Geophysical Research*, **110**, 1-13.

Millan, R., Mouginot, J. and Rignot, E. (2017). Mass budget of the glaciers and ice caps of the Queen Elizabeth Islands, Canada, from 1991 to 2015. *Environmental Research Letters*, **12**, 024016.

Mortimer, C., Sharp, M. and Wouters, B. (2016). Glacier surface temperatures in the Canadian High Arctic, 2000–15. *Journal of Glaciology*, **62**(235), 963-975.

Muller, F. (1962). Zonation in the accumulation area of the glaciers of Axel Heiberg Island, N.W.T., Canada. *Journal of Glaciology*, **4** (33), 302-311.

Partington, KC. (1998). Discrimination of glacier facies using multi-temporal SAR data. *Journal of Glaciology*, **44** (146), 42-53.

Pfeffer, T., Meier, M., and Illangasekare, T. (1991). Retention of Greenland runoff by refreezing: implications for projected future sea level change. *Journal of Geophysical Research*, **96** (C12), 117-22.

Radić, V. and Hock, R. (2010). Regional and global volumes of glaciers derived from statistical upscaling of glacier inventory data. *Journal of Geophysical Research*, **115**(F1).

Sharp, M., Burgess, D., Cogley, G., Ecclestone, M., Labine, C. and Wolken, G. (2011) Extreme melt on Canada's Arctic ice caps in the 21st century. *Geophysical Research Letters*, **38**, 1- 5.

Sylvestre, T., Copland, L., Demuth, M.N. and Sharp, M. (2013). Spatial Patterns of Snow Accumulation across Belcher Glacier, Devon Ice Cap, Nunavut, Canada. *Journal of Glaciology*, **59**(217), 874-882.

Ulaby, F., Moore, R. and Fung, A. (1986). Microwave remote sensing, active and passive. Reading, MA. *Addison-Wesley Publishing Co*. 3rd ed.

Wang, L., Sharp, M., Rivard, B. and Steffen, K. (2007). Melt season duration and ice layer formation on the Greenland ice sheet, 2000-2004. *Journal of Geophysical Research*, **112**(F4).

Wolken, G.J., Sharp, M. and Wang, L. (2009). Snow and ice facies variability and ice layer formation on Canadian Arctic ice caps, 1999-2005. *Journal of Geophysical Research*, **114**, 1-14.

The Cryosphere Discuss., https://doi.org/10.5194/tc-2018-250
Manuscript under review for journal The Cryosphere
Discussion started: 26 November 2018

The Cryosphere
Discussions
Open Access

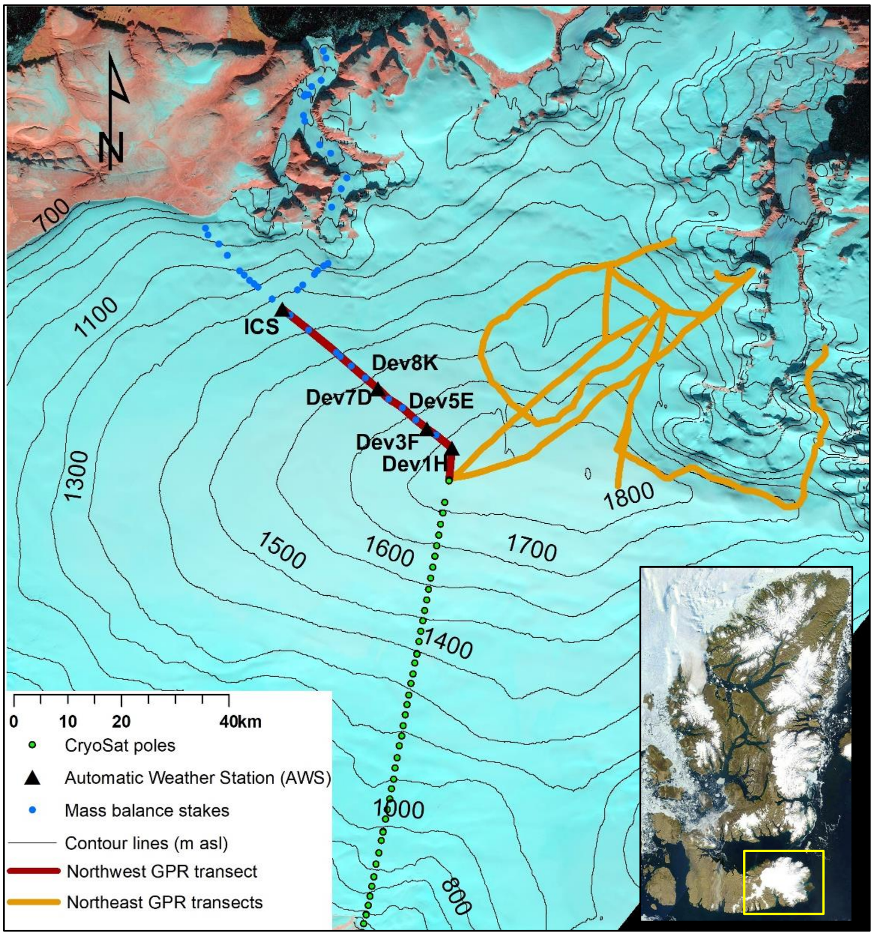

Figure 1. Landsat 7 image of Devon Ice Cap (September 14, 2002) with location of GPR transects, mass balance stakes, and automatic weather stations referred to in the text. Inset: location of Devon Ice Cap (in yellow) within the Canadian Arctic Archipelago; source: MODIS Rapid Response, NASA/GSFC.

The Cryosphere Discuss., https://doi.org/10.5194/tc-2018-250
Manuscript under review for journal The Cryosphere
Discussion started: 26 November 2018

The Cryosphere Discussions
Open Access

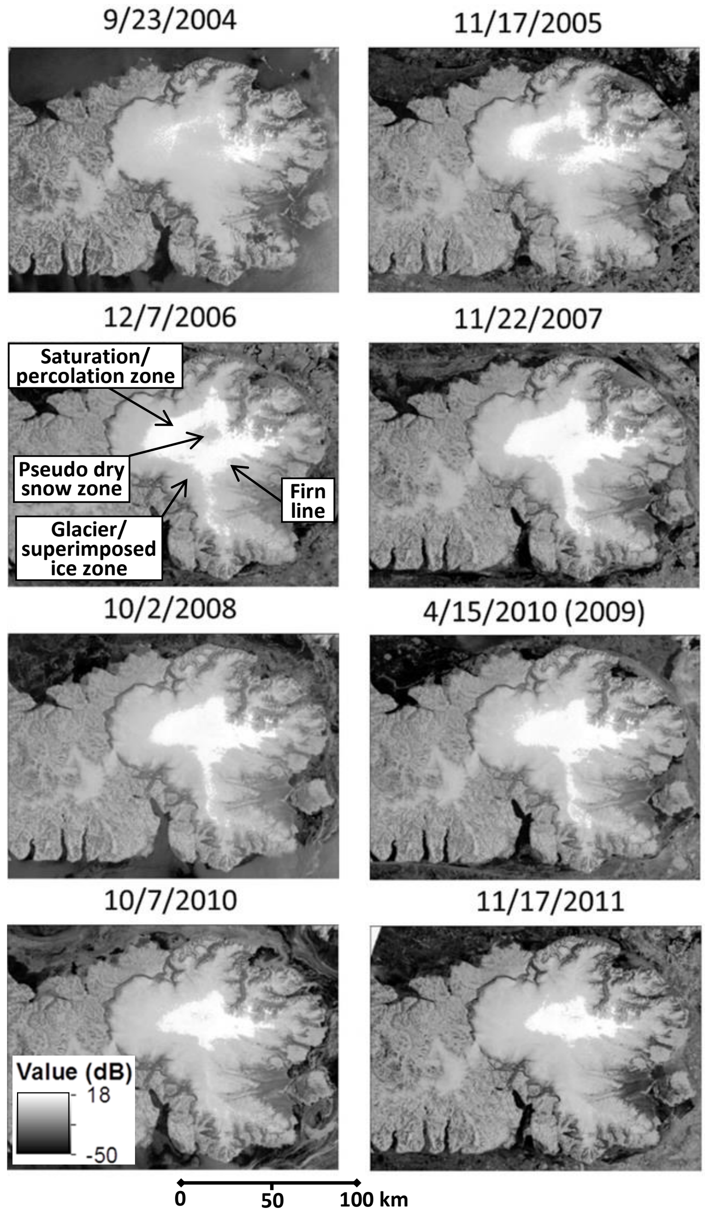

Figure 2. Post freeze-up Envisat ASAR WS imagery over Devon Ice Cap from 2004-2011. Areas near the ice cap summit with a low backscatter (grey) indicate the pseudo dry snow zone from 2004-2006. High backscatter areas (white) depict the saturation/percolation zone, with low backscatter showing the glacier ice/superimposed ice zone below this, with the firn line separating these regions. Images indicate glacier facies at the end of the previous summer, so the 4/15/2010 image reflects conditions from late summer 2009.

The Cryosphere Discuss., https://doi.org/10.5194/tc-2018-250
Manuscript under review for journal The Cryosphere
Discussion started: 26 November 2018

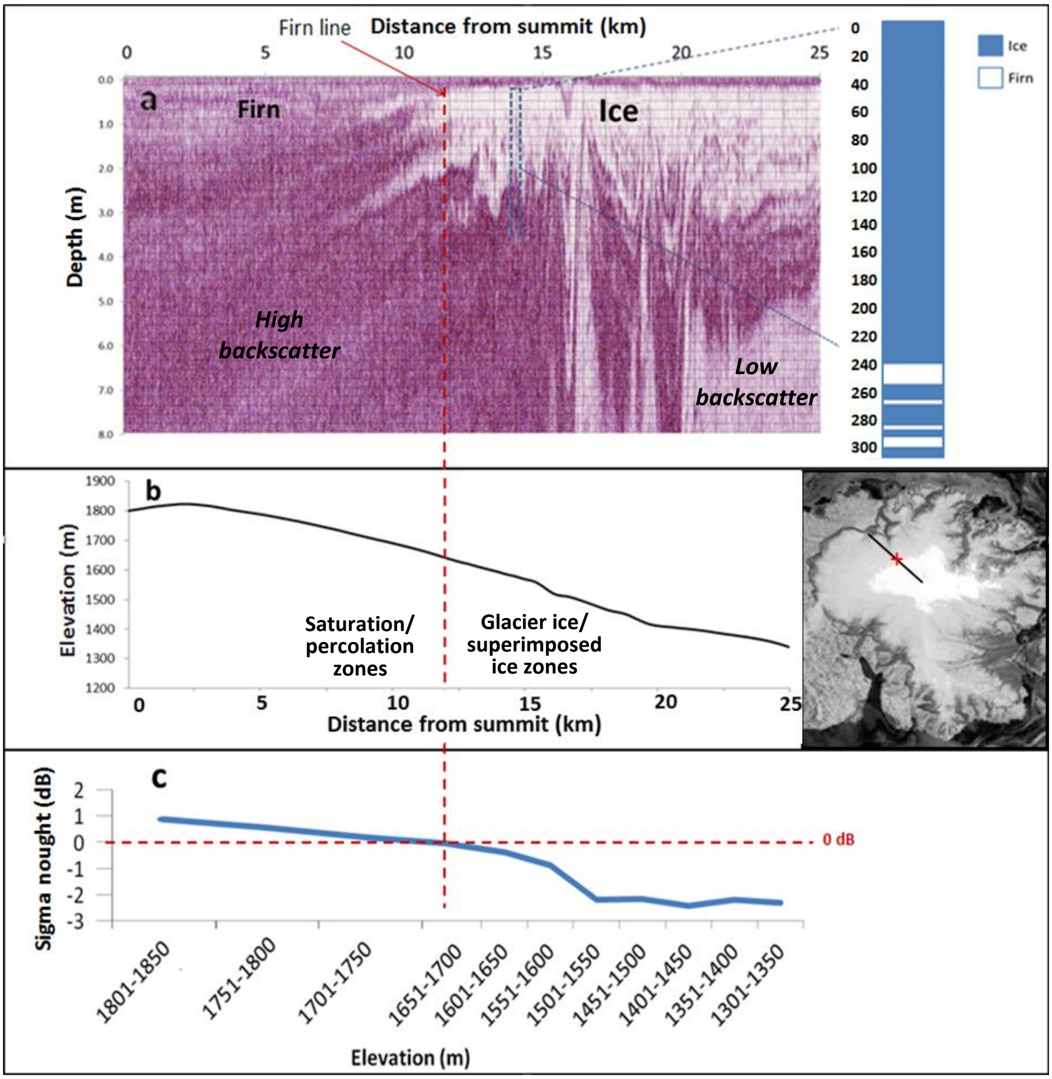

Figure 3. (a) May 2011 GPR radargram from the northwest transect, with Dev8K ice core (1557 m a.s.l.); (b) surface elevation profile for the GPR transect, with transect location marked in Envisat ASAR WS image from Oct. 7, 2010 (+ indicates location of firn line); (c) extracted sigma nought from the Oct. 7, 2010 Envisat image along the GPR transect.

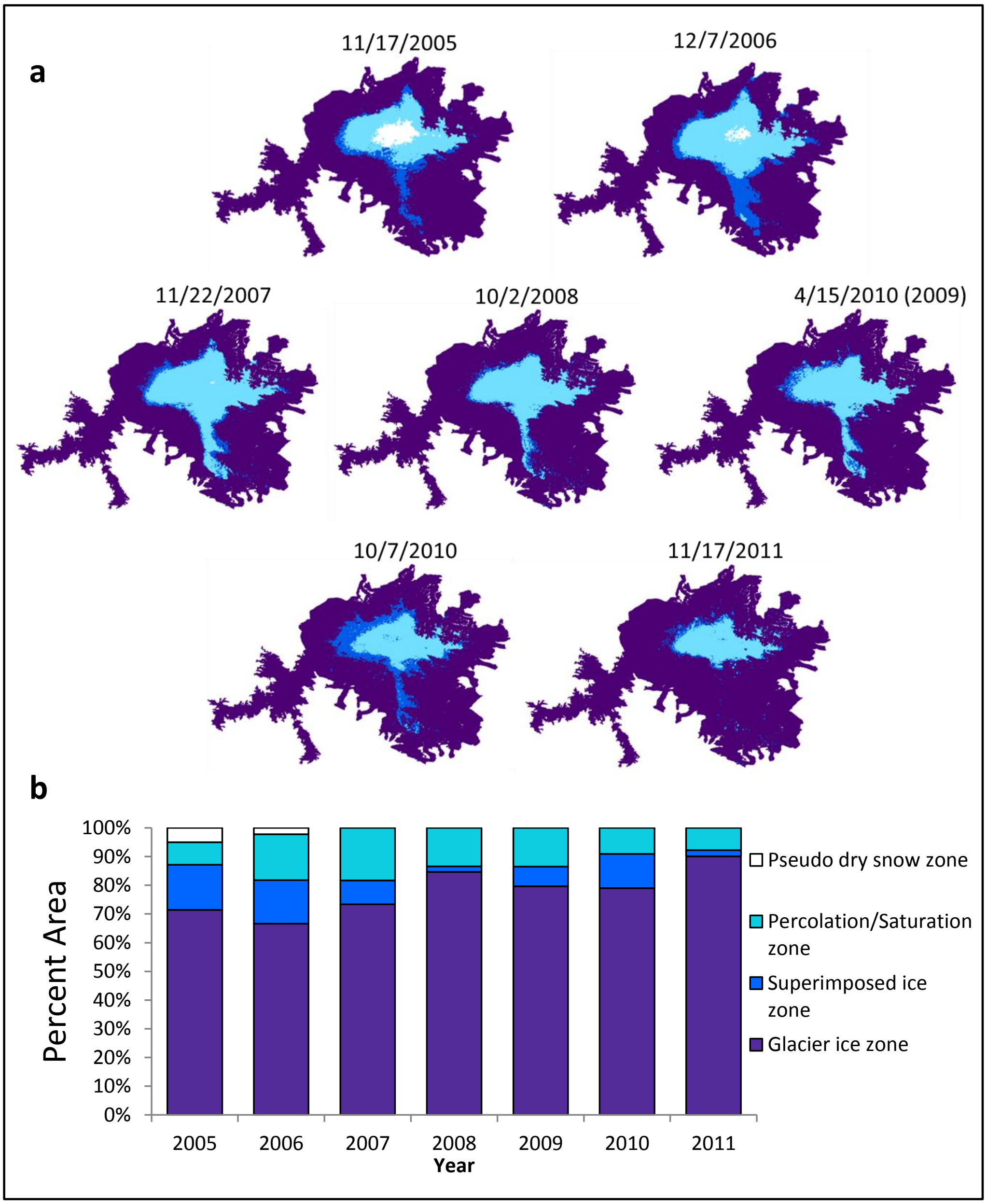

Figure 4. (a) Spatial extent and (b) percent area change of each glacier facies zone over Devon Ice Cap based on classification of Envisat ASAR Wide Swath mode imagery acquired from 2005 to 2011.

The Cryosphere Discuss., https://doi.org/10.5194/tc-2018-250
Manuscript under review for journal The Cryosphere
Discussion started: 26 November 2018

The Cryosphere
Discussions
Open Access

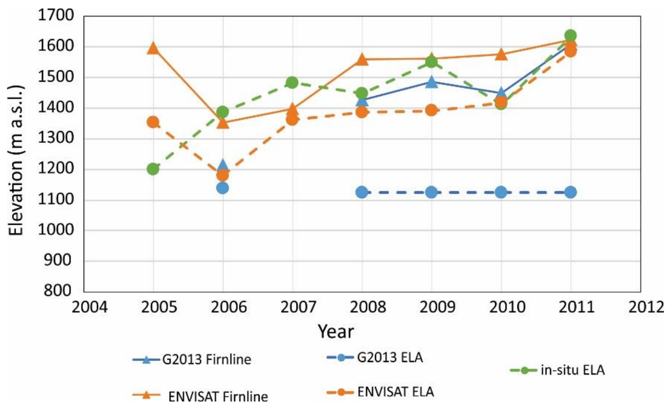

Figure 5. Comparisons between facies zone boundaries derived along the CryoSat transect in this study from Envisat imagery (ENVISAT Firnline, ENVISAT ELA), from GPR profiles by Gascon et al. (2013) (G2013 Firnline, G2013 ELA), and the in situ ELA derived from mass balance stake data along the CryoSat transect. Note that results from Gascon et al. (2013) were not available for 2007.

The Cryosphere Discuss., https://doi.org/10.5194/tc-2018-250
Manuscript under review for journal The Cryosphere
Discussion started: 26 November 2018

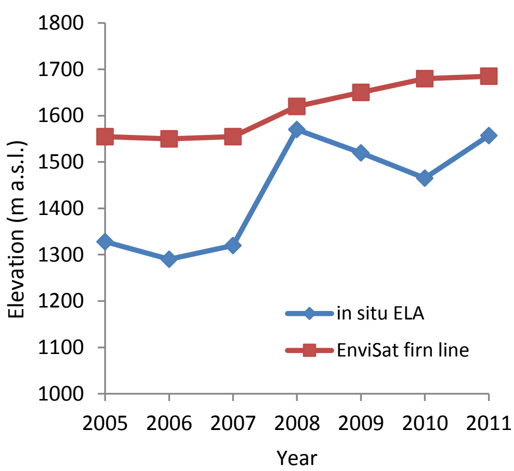

Figure 6. Firn line derived from Envisat ASAR WS mode imagery extracted along the location of the northwest transect on Devon Ice Cap, and the Equilibrium Line Altitude (ELA) derived from in situ mass balance measurements on the northwest transect from 2005-2011.

The Cryosphere Discuss., https://doi.org/10.5194/tc-2018-250
Manuscript under review for journal The Cryosphere
Discussion started: 26 November 2018

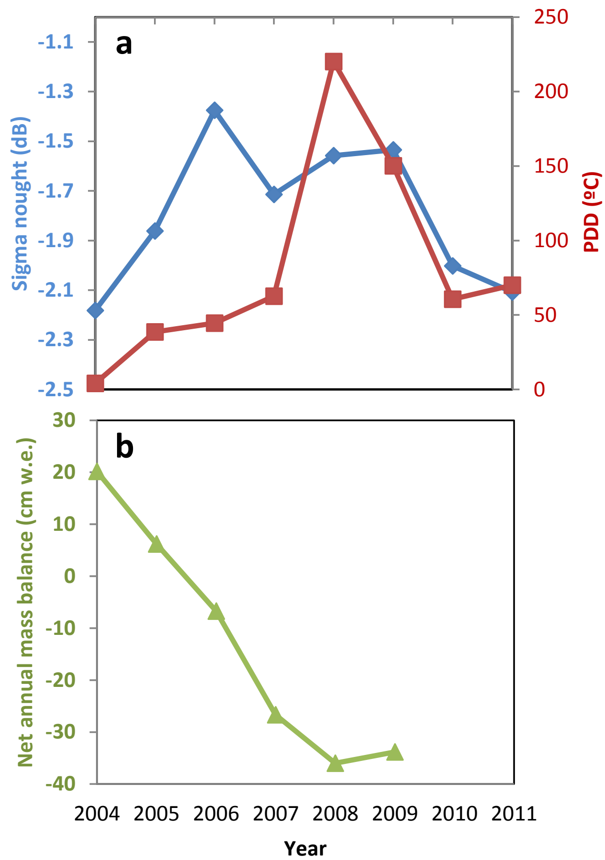

Figure 7. (a) PDD values recorded at ICS (1317 m a.s.l.) and sigma nought (σ^0) values extracted from the Envisat ASAR WS imagery averaged over the elevation range 1300-1350 m a.s.l. along the NW transect; (b) Net annual mass balance values at ICS (1317 m a.s.l.)

The Cryosphere Discuss., https://doi.org/10.5194/tc-2018-250
Manuscript under review for journal The Cryosphere
Discussion started: 26 November 2018

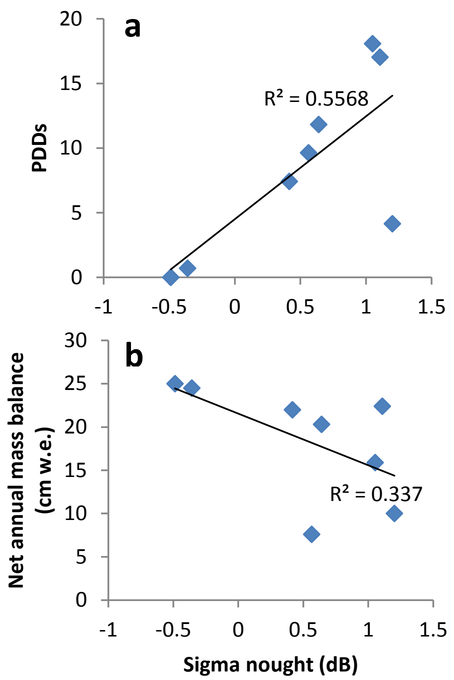

Figure 8. Relationship between the extracted 1750 – 1800 m sigma nought (σ^0) values along the NW transect from 2005-2011 and (a) PDDs, (b) net annual mass balance.